NANOSCALE SEMICONDUCTOR-CATALYST CONTACTS FOR WATER SPLITTING PHOTOANODES

by

ADRIAN GORDON

A THESIS

Presented to the Department of Chemistry
and the Robert D. Clark Honors College
in partial fulfillment of the requirements for the degree of
Bachelor of Science

June, 2019

An Abstract of the Thesis of

Adrian Gordon for the degree of Bachelor of Science
in the Department of Chemistry to be taken June, 2019

Title: Nanoscale semiconductor/catalyst interfaces for water splitting photoanodes

Approved: ______________________________________

Shannon W. Boettcher

The development of stable and efficient photoanodes for the oxygen evolution reaction (OER) remains a barrier to the realization of commercially viable photoelectrochemical cells. Photoanodes are often fabricated by depositing a thin metal/metal-oxide protection layer on silicon. Studies have shown thinner protection layers correlate with higher performing photoanodes. Additionally repeated electrochemical cycling has shown to enhance performance of photoanodes. Both these phenomena have been hypothesized to result from generation of a spatially inhomogeneous interface following oxidation of the redox active catalyst. The effective barrier height of low barrier height silicon-metal contacts becomes enhanced by surrounding semiconductor-metal oxide contacts, in what is known as the ‘pinch off effect’. In this work, nickel nanoislands which exhibit the pinch off effect are intentionally fabricated using an electrodeposition technique on a silicon photoanode. The efficiency of nanoisland-decorated devices is evaluated using cyclic voltammetry. In addition, we show that electrodeposited contacts can be protected with additional nickel, without compromising their rectifying properties.

Acknowledgements

I would like to thank my thesis committee for making this work possible. Professor Shannon Boettcher, thank you for providing me the opportunity to work in your lab, and for being an exemplary scientist. Forrest Laskowski, thank you for your mentorship and for teaching me so much about my thesis topic. Professor Casey Shoop, thank you for your kind support throughout my college career.

I would also like to thank all members of the Boettcher group. Thank you for making my experience in the lab a happy one. Finally, thank you to my parents, Matt and Julie, for your continuous love and support.

Table of Contents

List of Figures

Introduction

Photo water splitting

Hydrogen, when chemically reacted with oxygen to produce water, is a clean, renewable fuel source. However, 95% of hydrogen currently produced in the United States is made through the steam reformation of natural gas, a process which releases carbon dioxide to the atmosphere.1 In order to realize a sustainable hydrogen fuel economy, a clean method for the production of hydrogen needs to be developed. Splitting water (H2O) to produce hydrogen along with oxygen using electricity, a process known as water electrolysis, is one promising method:

$$H_2O \rightarrow H_2 + \frac{1}{2}O_2 \tag{1}$$

Water splitting is an uphill reaction, which means the products, hydrogen and oxygen in their diatomic gas form, are less energetically favored than the reactant, water. A driving force is needed to break the covalent bonds of water. In electrolysis, electricity from an external source provides the driving force. To be precise, a potential difference of at least 1.23 V must be applied to the two electrodes to split water, although various energetic losses may be present which increase the required driving force.

Electrochemical processes, like water splitting, occur when molecules in solution undergo chemical reactions on solid electrodes. Electrochemical reactions are always oxidation-reduction reactions, which means they involve the transfer of electrons from one species to another. Redox reactions can be split into two half reactions, one involving the species that loses electrons and the other involving the species that gains electrons. For example, the reaction for water splitting consists of two half reactions:

(2) $$2H_2O \rightarrow 4H^+ + O_2 + 4e^-$$

(3) $$2H^+ + 2e^- \rightarrow H_2$$

Notice that in reaction (2), oxygen loses electrons; this is an oxidation reaction called oxygen evolution (OER) and takes place at an electrode called the anode. In reaction (3) protons gain electrons; this is a reduction reaction called hydrogen evolution (HER) and takes place at the cathode. Some reactions occur spontaneously, in which case electrons released by an oxidation reaction at the anode electrode flow through a circuit to the cathode where they are consumed in a reduction reaction. An example of this type of cell is a battery, which harnesses spontaneous reactions to create electrical energy that can perform useful tasks. Other reactions, such as water splitting, are not spontaneous. A voltage must be applied across the electrodes to drive non-spontaneous chemical reactions. An analogy to voltage is the gravitational potential energy that makes water flow over a water wheel. The potential energy difference must be large enough to make the desired process occur—in the case of the watermill producing mechanical energy in the form of a spinning wheel, and in the case of water splitting producing chemical energy in the form of oxygen and hydrogen bonds.

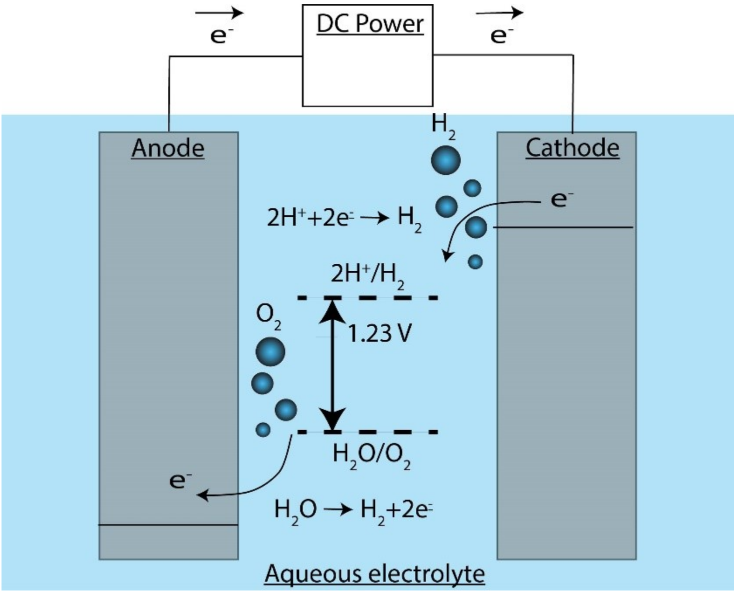

Figure 1. An illustration of a water electrolysis cell. The dashed lines show the redox potentials for water splitting. A DC power source provides the required potential difference to the electrodes. Dissolved salt ions (not shown) form an aqueous electrolyte that allows charge to flow through water.

The voltage required to perform a non-spontaneous reaction is determined by the energy difference between the reactants and products of a reaction. Theoretically, the potential difference required to split water is 1.23 V, corresponding to a free energy of 237 kJ/mol. In practice the potential required is often greater than the theoretical prediction due to the sluggish nature of the oxygen evolution reaction (OER). The voltage is sometimes supplied by a source external to the water splitting cell, for example the grid, a battery, or a photovoltaic. Alternatively, the electrodes in the cell may directly absorb energy from incident sunlight and use this energy to drive water electrolysis.[2] In this system, the voltage needed to drive water splitting is provided by the sun and electrical gradients that arise from equilibration between the electrode and electrolyte. Devices that utilize sunlight for water splitting are known as photoelectrochemical (PEC) cells.

PEC cells require a material that can absorb sunlight and produce electrical energy. Semiconductors are a class of materials that exhibit many ideal properties for solar-to-electricity energy conversion. Semiconductors consist of atoms arranged in a three-dimensional crystal lattice. Quantum mechanics has allowed scientists to understand what happens when the individual atomic orbitals of atoms combine in lattice structures.[3] In semiconductor materials, atomic orbitals combine to form an equal number of delocalized energetic states, all at slightly different energy levels. For lattices composed of a large number of atoms, these different energy levels are so close together that the delocalized energetic states can be thought of as forming continuous bands of energy. A key property of semiconductors is the presence of two distinct bands of energy separated by a *band gap* E_g. Electrons never occupy an energy within the band gap. The lower energy band is called the valence band and the upper energy band is called the conduction band. At room temperature many electrons remain in the valence band. However incident light may excite electrons from the valence band to the conduction band, if the energy of the light is equal to or greater than the semiconductor band gap. These excited electrons have a higher potential energy than the electrons in the valence band. Another useful term to introduce is the hole, which is the vacancy left in the valence band when an electron is excited to the conduction band. Electron holes move freely in the valence band, just as electrons move in the conduction band.

A photo water splitting device harvests photo-generated electrons and holes from a semiconductor and uses them for the water splitting reaction. Photo-generated electrons flow towards the cathode for hydrogen reduction and the holes flow the opposite direction, to the surface of the anode for water oxidation. Unlike water electrolysis, where the driving force for the reaction is provided solely by an external source, in a PEC water splitting device the excitation of electrons to the conduction band of the semiconductor contributes ideally all of the driving force required for water splitting.

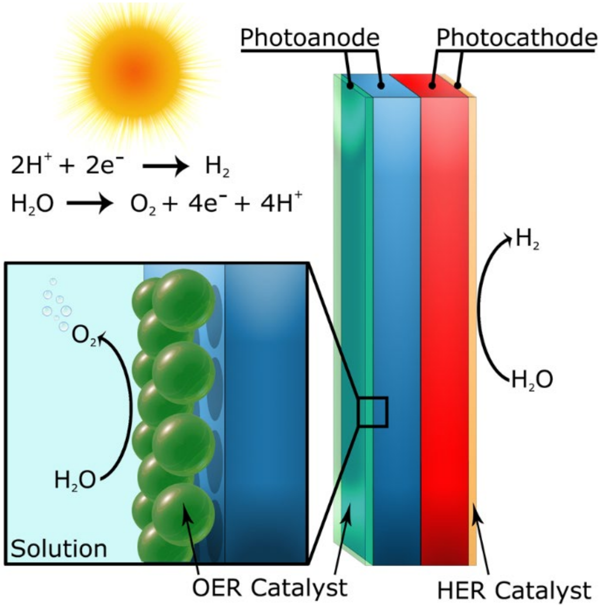

Figure 2. An illustration of a photoelectrochemical cell. Oxygen is evolved at the photoanode and hydrogen is evolved at the photocathode.

In 1972 Fujishima and Honda reported photo induced water oxidation on a titanium dioxide electrode with only a small external bias applied.[4] Since then interest in PEC water has exploded. Cell designs have utilized a range of semiconducting materials including Si, Fe_2O_3, $BiVO_4$, and WO_3 semiconductors, as well as a variety of different geometries that range from monolithic devices composed of one electrode which performs both hydrogen and oxygen evolution to devices composed of two photoactive electrodes.[2] In the titanium dioxide cell described by Fujishima, the interface between the semiconductor and electrolyte alone provides the electric field needed to separate charge. However, semiconductors that easily corrode in electrolyte, such as silicon, are often used for photo water splitting, due to their superior light absorbing properties. These corrosion prone semiconductors need a surface protection layer to achieve long term stability for water splitting. Metal or metal oxide layers are often deposited onto semiconductor surfaces to both preserve the semiconductor from corrosion and catalyze the water splitting reactions.[5,6]

A key factor that limits device performance is the efficiency with which the two charge carriers, electrons and holes, are separated. Recombination of electrons and holes reduces the number of charge carriers available for the water splitting reaction, thus lowering the overall efficiency of the cell. PEC cells must have a means of separating charge. Equilibration processes at the semiconductor-metal and semiconductor-solution interfaces provide the free energy gradients needed to separate charge carriers. The next section of the thesis will discuss these equilibration processes.

Schottky diodes and the pinch off effect

When two phases make contact, they electrochemically equilibrate. Equilibration can generate strong electric fields advantageous in PEC cells. For photochemical water splitting, we are most interested in contacts formed between semiconductors, metal or metal oxide electrocatalysts and solution. In this thesis, the equilibration process between semiconductor-metal contacts will be discussed, although the equilibration between semiconductors and solution behave similarly.

The process of equilibration is determined by the electrochemical potentials of the phases in contact. Electrochemical potential is a measure of the stability of a chemical species in a given environment, considering short range interactions with other chemicals as well as long range electrical potential gradients.

The more positive the electrochemical potential in an environment, the more favorable it is for a species to exist there; hence species move from regions of lower to higher electrochemical potential. The electrochemical potential of a semiconductor can be tuned by doping (chemically substituting atoms) the semiconductor lattice with atoms of higher or lower valency. Doping with higher valent atoms will lower the electrochemical potential while lower valent atoms will do the opposite. Upon equilibration with a n-type semiconductor, one doped with higher valent ions, electrons spontaneously leave the silicon and enter the metal until the electrochemical potential of the two phases becomes equal. In this case, the electrochemical potential of the semiconductor increases until it reaches the electrochemical potential of the metal.[7] The origin of this increase is discussed subsequently.

As a consequence of charge transfer, charge neutrality in the semiconductor and the metal are disrupted. The electrons leaving the semiconductor leave behind positively charged atoms in the crystal structure. Since dopant atoms are more easily ionized than silicon atoms, electrons are preferentially pulled from dopant atoms. The low concentration of dopant atoms in the lattice necessitates that electrons are pulled from a depth greater than one atomic layer of the silicon. The depth to which electrons are pulled from the semiconductor is known as the depletion width.

a) Low Barrier Height Contact

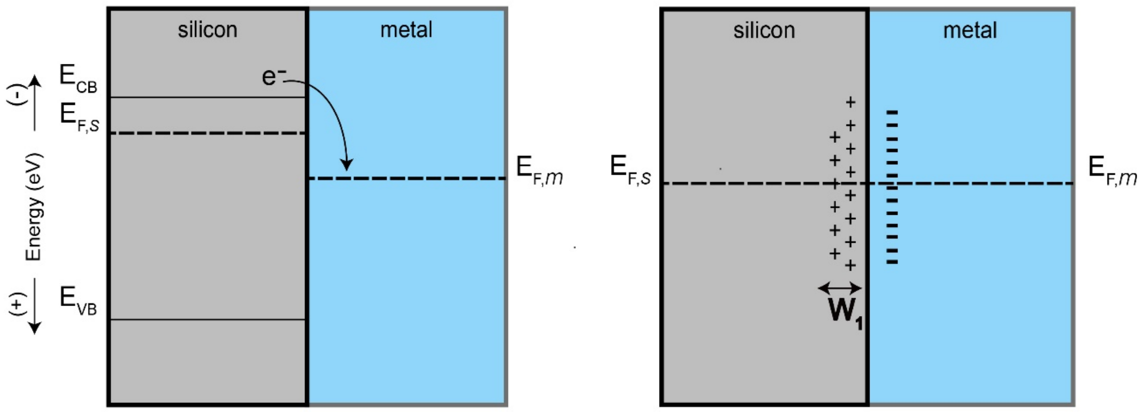

b) High Barrier Height Contact

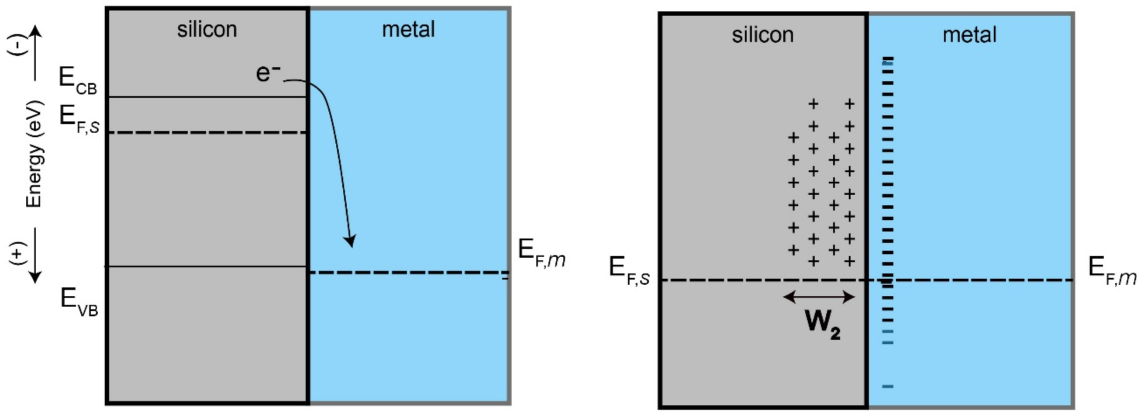

Figure 3. Diagram showing the equilibration process between n-type silicon and two metals with different electrochemical potentials. E_{VB} and E_{CB} denote the energies of the valence and conduction bands respectively. $E_{F,S}$ and $E_{F,M}$ denote the energies of the Fermi levels of the semiconductor and metal, which are equivalent to their electrochemical potentials. In image b) the electrochemical potential difference between the silicon and metal is greater; hence more charge must flow across the interface to equilibrate, increasing the depletion width and the electric field strength at the interface.

The build-up of charge at the interface creates an electric field. To understand this electric field, consider a negatively charged electron as it moves moves along the z-axis perpendicular toward the semiconductor surface. When the electron is at a distance from the semiconductor surface greater than the depletion width, the electron does not experience a net electrostatic force, because the negative charges on the metal side interface are screened by an equal number of positive charges in the semiconductor's depletion region. However, as the electron moves into the depletion region, there are fewer and fewer positive charges between it and the negative charges in the metal. Therefore, the electron feels repulsed by the electrons in the metal and experiences an electric field. As the electron moves closer to the interface, it feels more and more repelled by the negative charges in the metal. Work must be done to move the electron. In other words, the electric field creates an energy barrier that the electron must overcome to cross the interface. The probability that an electron will cross the interfaces decreases as a function of the height of this energy barrier. This electric field is also what equilibrates the electrochemical potential of the semiconductor with the metal.

The presence of the energy barrier creates a junction that inhibits electron flow in primarily one direction—from the semiconductor to the metal. Junctions that preferentially allow electrons to flow in one direction are said to exhibit rectification. A metal-semiconductor contact that exhibits rectifying properties is called a Schottky diode. Figure 4 shows some key parameters of Schottky diodes. The most important is the barrier height $q\phi_b$. The Schottky barrier height (SBH) is defined as the energy barrier an electron must overcome to travel from the metal to the semiconductor. An increase in this barrier proportionally increases the barrier for electrons traveling from the semiconductor to the metal. The greater this barrier is, the less likely electrons will flow to the interface. The Schottky barrier height is extremely important for solar water splitting cells because it provides the means of separating charge in the cell. If photo-generated electrons in the semiconductor cross the interface, they often recombine with holes, decreasing the number of charge carriers available to participate in electrochemical reactions like water oxidation. Therefore, the presence of larger barrier heights at the interface lowers the rates of recombination and improves the efficiency of photoelectrochemical cells.[7]

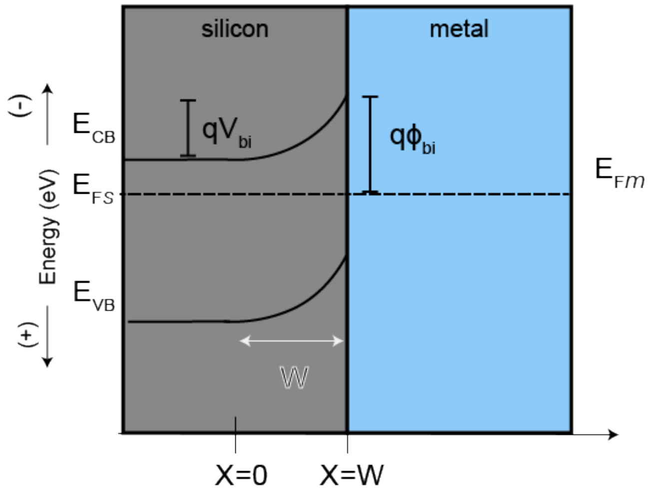

Figure 4. The energy levels at semiconductor-metal Schottky diode. The built-in potential V_b is the difference between the electric potential in the bulk semiconductor and at the interface. V_n denotes the difference between the Fermi level and the conduction band of the semiconductor. The barrier height ϕ_b is defined as the difference between the equilibration Fermi level and the bottom of the conduction band. Parameters in volts are multiplied by the elementary charge q to obtain energies in units of electron volts.

High barrier height junctions are formed between a semiconductor and a metal that have a large difference in electrochemical potential. In other words, high barrier heights occur when it is significantly more favorable for electrons to be in the metal. A property that measures how stabilizing a material is for electrons is the *work function*, defined as the energy required to remove an electron from a metal.

For a given n-type semiconductor, there are two options for the formation of highly rectifying junctions. One is to coat the semiconductor with a high work function metal catalyst. However, it is difficult to find materials that have high work functions and are catalytically active. Another option is to engineer a junction that combines catalytically active materials with high work function materials that are not necessarily good catalysts, creating a junction that exhibits both high activity for the OER reaction and high rectification.

This second device design depends on the formation of spatially inhomogeneous metal semiconductor junctions, in which low SBH contacts are surrounded by neighboring high SBH contacts. Traditionally patches with different barrier heights were modeled as independent contacts which do not interact with one another.[8] However, it was found that this model fails to predict important experimental data. When the areas of neighboring contacts with different barrier heights become very small, the behavior of each contact cannot be considered independently. Specifically, when a low SBH contact is surrounded by high SBH contacts, the contact is "pinched-off" i.e. it experiences a higher effective barrier height than it normally would. The pinch-off effect describes the enhancement of the barrier height behind a spatially confined patch, due to surrounding high barrier height contacts.

Physically, a low barrier height contact becomes "pinched-off" when the depletion regions of surrounding high barrier height contacts overlap, raising the energy barrier an electron must overcome to cross the semiconductor-metal contact at the pinched-off contact. Mathematically, the electrical potential behind a pinched-off patch can be modeled as a point contact. We can express the potential as modification to the potential behind a homogeneous contact. Similarly, the electric current that flows through a pinched-off contact can be understood as a modification to the ideal diode equation which describes the transport of electrons across a homogeneous Schottky diode as a function of applied voltage. Pinch-off occurs when

$$R_o < \frac{W\Delta}{2V_b}, \tag{4}$$

where R_o is the radius of the contact, W is the depletion width behind the high barrier height contact, Δ is the difference between the barrier heights of the high and low barrier height regions.[9] As can be seen from the equation, pinch-off is more likely to occur when the radius of the contact is smaller.

The pinch-off effect has received some attention in the literature in relation to photoelectrochemical cells. Inhomogeneous nickel semiconductor junctions exhibiting the pinch off effect have been fabricated using nanolithography methods, with suggested applications to photo water splitting devices.[9] In addition, it has been hypothesized that efficiency enhancements of thin thermal or electrodeposited metal layers on silicon photoanodes arise from incidental generation of spatially inhomogeneous interfaces which experience the pinch off effect.[10,11] The goal of this thesis is to intentionally fabricate pinched-off nanocontacts using electrodeposition methods. We aim to demonstrate how precise control of the geometry of the semiconductor-metal interface can be used both as a tool to fundamentally understand the semiconductor metal interfaces and as a way to design more efficient photoanodes for photo water splitting devices.

Methods

First, the basic methods used in this thesis project are described in general terms. Then the specific experimental procedures used for this work are described in detail.

Explanation of methods

Three electrode set-up

When doing electrochemistry, we are generally interested in the behavior of a single electrode/electrolyte interface. However, it impossible to measure a single interface in isolation.[12] For electrochemical measurements the electrode of interest, called the working electrode is placed in a three-electrode cell, which also contains a counter electrode and reference electrode. The working electrode is the electrode on which the chemical phenomena of interest occurs. During an electrochemical experiment in which voltage is controlled, it is the potential applied to the working electrode that is controlled. The reference electrode provides a known potential against which changes in the potential of the working electrode can be measured. The potential of the reference electrode remains constant during the experiment. The counter electrode completes the electric circuit in the cell; it passes the same amount of current as the working electrode, but with the opposite sign. Using a three electrode setup, we can perform a number of electrochemical techniques, including electrodeposition and cyclic voltammetry.

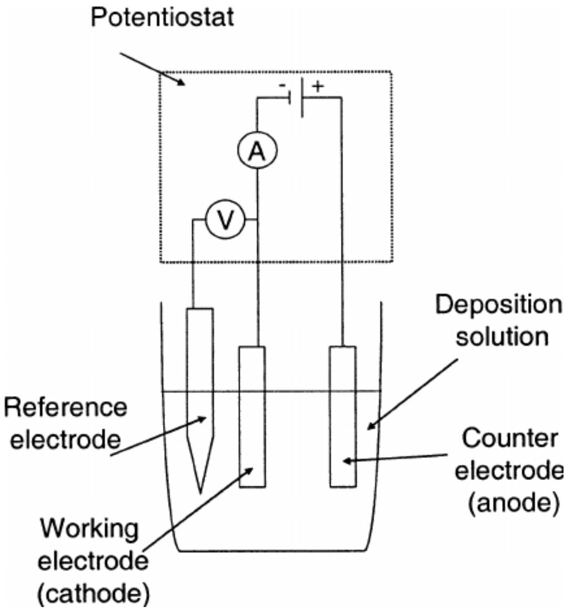

Figure 5. Three electrode set up connected to a potentiostat, an electronic device that maintains the potential of the working electrode with respect to the reference electrode.

Electrodepostion

To fabricate catalyst nano-islands on a silicon substrate, an electrodeposition technique was used. In electrodeposition, a negative potential is applied to an electrode immersed in a salt solution containing metal cations. The cations are reduced and deposited onto the electrode. For example, in a nickel deposition, dissolved Ni^{2+} (aq) ions are reduced to Ni (s) at the electrode.

Cyclic Voltammetry

In cyclic voltammetry, the voltage applied to an electrode is swept between two potentials and the current response of the electrode is measured. The applied potential is swept linearly versus time.[12] Cyclic voltammegrams (CVs) consist of a forward sweep, during which the potential increases over time to its maximum and a reverse sweep, during which the potential decreases back to its minimum. CVs allow one to observe the potential at which the oxygen evolution reaction occurs, called the photocurrent onset potential. Generally the photocurrent onset potential is found by locating the potential at which the CV forward sweep begins to increase exponentially. CVs also provide information about behavior of surface catalysts. As shown in Figure 1, oxidation of redox active catalysts during the forward sweep and reduction of the catalysts in the reverse sweep cause small peaks in the current response.

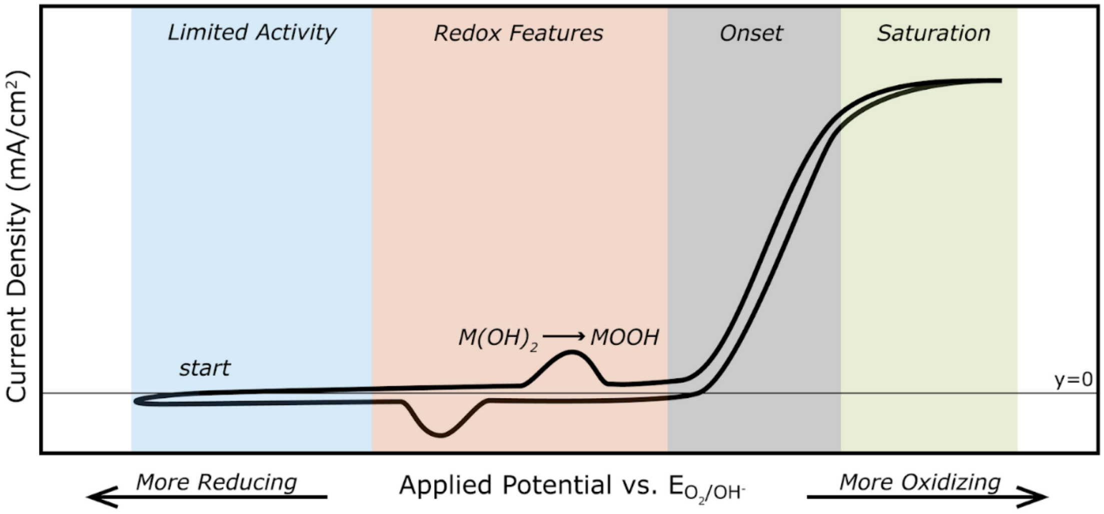

Figure 6. The typical shape of a cyclic voltammegram collected on a silicon based photoanode under illumination. Both the forward and reverse sweeps are shown. At more reducing applied potentials the current passed at the photoanode is low because there is limited OER activity. As the applied potential increases, transfer of holes from the silicon to the surface catalyst transforms the catalyst to its oxidized form. When the applied potential reaches the OER onset potential, OER occurs, leading to the exponential increase in current passed at the photoanode. The current increases with applied potential until it becomes limited by the number of photo-generated holes in the silicon, which results in current saturation.

Atomic Force Microscopy

Atomic force microscopy is a technique used to gain detailed topographic images of surfaces, with resolutions down to fractions of a nanometer. A sharp tip at the end of a cantilever is raster scanned across a surface. Forces such as Van der Waals forces, dipole-dipole interactions etc. between the tip and the sample cause the tip to deflect away from the sample, changing the amplitude of the tip's oscillation's over the surface. From these deflections in amplitude, the instrument constructs a height map the surface.[13]

Procedures

Phosphorous-doped n-Si [100] (0.65 - 0.95 ohm·cm) wafers (University Wafer) were cut into approximately 1 × 1 cm squares. To remove oils and organic residues on the surface of the wafers, they were sonicated for 10 min each in acetone, isopropyl alcohol, and water (18.2 MΩ·cm). To further remove metals and organic contaminants, the wafers were placed in a highly oxidative piranha solution (~100 °C – 3:1 by volume conc. aq. H_2SO_4 : 30% aq. H_2O_2 – both from Fisher Chemical) for 30 min. The wafers were turned into full electrodes by forming an ohmic back contact to the wafers. Ga-In eutectic (≥99.99%, Sigma Aldrich) was applied to the backside of the wafers and one end of a Sn-Cu wire was affixed within the Ga-In eutectic, using hot glue. The Sn-Cu wire was placed in a glass tube and the back contact insulated further with hot glue. Before performing depositions on the electrodes, they were submerged in a buffered hydrofluoric acid etching solution (20:1 buffered oxide etch, J. T. Baker) for 2 min, in order to remove the native silicon dioxide on the wafers. Nickel was deposited on the silicon wafers using an electrodeposition technique reported by Loget et al.[14] The nickel depositions were performed in a three electrode cell consisting of the working electrode, a Pt coil counter electrode and an Ag/AgCl reference electrode, immersed in a 0.01 M $NiCl_2$ + 0.1 M H_3BO_3 solution. A potential of -1.5 V vs. $\mathcal{E}_{Ag/AgCl}$ was applied using a BioLogic SP200 potentiostat.

Photoelectrochemical experiments were performed in a three electrode cell consisting of working electrode, Pt coil counter electrode, and Ag/AgCl reference electrode immersed in 1 M potassium hydroxide (KOH). The electrodes were activated via 60 voltammogram cycles in electrolyte solution under 100 mW cm^{-2} of solar simulation (Abet Technologies model 10500). The potential ranges used for activation depended on the activity of the photoanodes. The potential minimum was chosen cathodic of the catalysts redox peak and the potential maximum in saturation current region.

Atomic force microscopy images were obtained on a Bruker Dimensional Icon AFM in imaging mode and using conductive tips (SCM-PIT-V2).

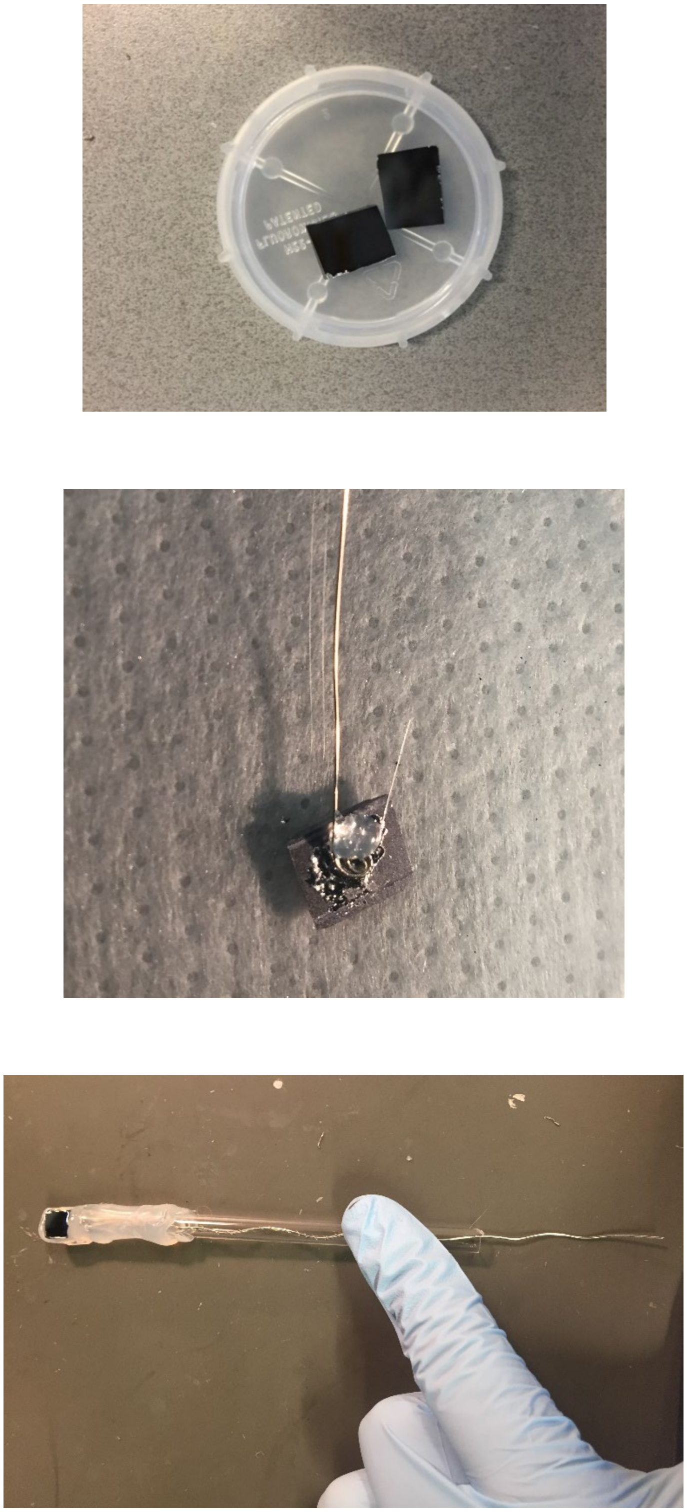

a)

b)

c)

Figure 7. Electrode preparation a) Silicon wafers before cleaning. b) Back contact on wafer formed using Ga-In eutectic and a Cu-Sn wire. c) Fully made electrode.

Results and Discussion

Following methods described above, well-defined, spherical nickel islands were deposited on a silicon substrate. The deposition time was varied to control the size of the deposited islands. Using atomic force microscopy to image the electrodeposited surfaces, it was found that a 5 second deposition produced nickel islands from 40-140 nm in diameter, while a 60 second deposition produced islands 250-400 nm in diameter.

Since the pinch-off effect acts more strongly on contacts of smaller size, we expect that photoanodes electrodeposited for shorter periods of time should exhibit higher efficiencies. To evaluate the efficiencies of the photoanodes, we used cyclic voltammetry (CV) analysis. First the photoanodes deposited with nickel for 5s, 10s, and 60s were cycled between an oxidizing and reducing potential in a three-electrode set up for up to 60 cycles under 1 sun illumination, a process we refer to as activation. The electrolyte used was 1 molar potassium hydroxide (KOH). Following activation, the CV response was collected on each photoanode. The CVs confirm our expectations that the electrodes with smaller islands perform significantly better. The photoanode deposited with nickel for 5 seconds shows a photocurrent onset potential ~300 mV more negative than the photoanode deposited for 60 seconds and ~150 mV more negative than the photoanode deposited for 10 seconds, demonstrating that oxygen evolution requires a significantly smaller energy input to proceed on the photoanode decorated with smaller islands – consistent with a semiconductor/metal interface that is more charge selective.

The superior performance of the photoanode with smaller nickel islands likely results from the formation of pinched-off contacts via the partial conversion of the deposited nickel to nickel-(oxy)hydroxide, $Ni(OH)_2$/NiOOH, during photoelectrochemical cycling. As the voltage is swept from a reducing to oxidizing potential, some of the nickel on the photoanode surface is oxidized from its reduced nickel hydroxide ($Ni(OH)_2$) form to its oxidized form NiOOH. The growth of a NiOOH layer likely occurs at the edges of nickel islands, where the nickel is exposed to solution, while a Si-Ni contact remains at the center of the island. Energy dispersive x-ray analysis (EDX) results have confirmed that oxygen becomes increasingly incorporated in the outer layer of the electrodeposited nickel islands during activation, suggesting the presence of NiOOH.[15] Since NiOOH has a large work function, we expect it forms a high barrier height contact with the silicon, which has been confirmed with impedance analysis. The high barrier height NiOOH-silicon contact surrounding the low barrier height Ni-silicon contact thus creates a pinched off junction. The islands formed in the 60s deposition most likely do not experience the pinch off effect, due to their large size. For the barrier height of 0.93 eV calculated for a NiOOH-silicon contact, pinch-off effect occurs when island's radii are below 142 nm. Hence, the majority of the islands formed in the 60s deposition are not pinched-off.

a)

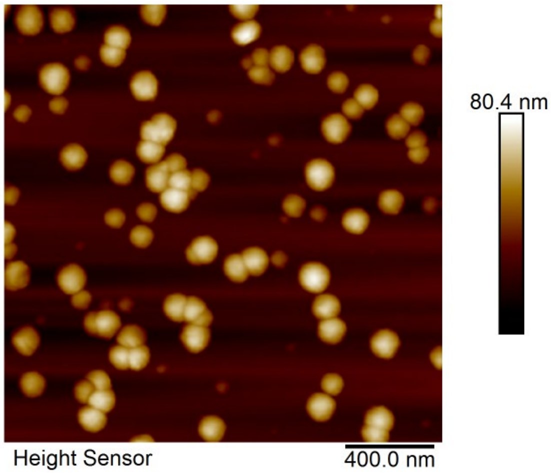
80.4 nm
Height Sensor
400.0 nm

b)

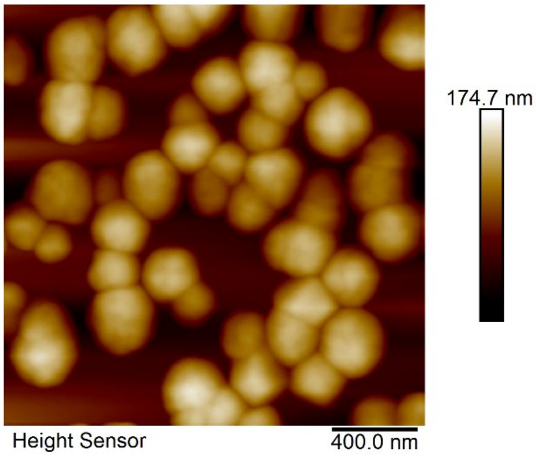
174.7 nm
Height Sensor
400.0 nm

c)

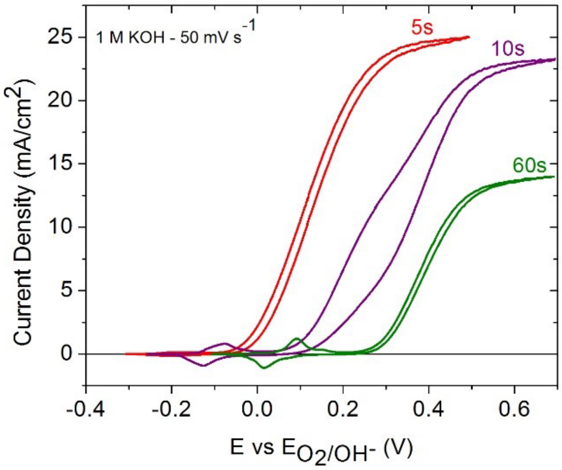
1 M KOH - 50 mV s^{-1}
5s
10s
60s
Current Density (mA/cm^2)
25
20
15
10
5
0
-0.4
-0.2
0.0
0.2
0.4
0.6
E vs E_{O_2/OH^-} (V)

d)

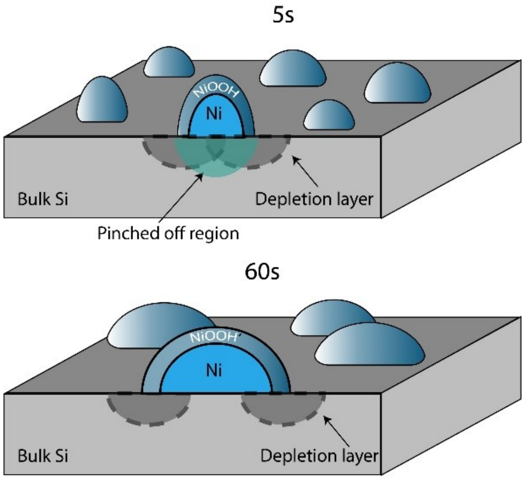

Figure 8. Comparing photoanodes with different island sizes. a) AFM image of photoanode surface after 5s nickel deposition. b) AFM image after 60s deposition. c) CV response after activation with 60 light cycles of the 5s depostion, 10s deposition and 60s deposition photoanodes d) Illustration of pinch-off at nickel islands. Pinch-off does not occur for larger islands (radii>142 nm).

The dramatic correlation between photocurrent onset potential and nickel island size illustrates the importance of pinched-offed junctions in the design of efficient photoanodes. However, small nanocontacts such as the nickel islands described above leave the surface of the photoanode relatively unprotected from the corrosive electrolytes often used for OER. The activity of islands can be compromised in two ways: (1) etching of the silicon beneath the nickel islands which causes the islands to detach from the surface and (2) complete conversion of the Ni to NiOOH which is solution permeable and allows the silicon to react and form a non-conducting oxide (SiO_2). To prolong the stability of photoanodes, new surface geometries must be developed which protect the silicon from electrolyte while also preserving pinched-off junctions. To illustrate the viability of this concept we used the nickel electrodeposition to fabricate pinched-off junctions, and then electrodeposited additional nickel over them as a protection layer. First, nickel was deposited for 5s to form nickel islands as previously discussed. Then the photoanode was cycled in potassium hydroxide electrolyte for approximately 60 cycles in order to oxidize the nickel and create the pinched-off junctions. After the electrode had been fully activated and the photoelectrochemical activity recorded, we performed a second 5s nickel electrodeposition on the same electrode and again measured the photoelectrochemical activity post activation. The second 5s electrodeposition did not cause the photocurrent onset potential to change significantly, shifting it only about 10 mV more positive (Figure 9a). This is a relatively small shift in photocurrent onset compared to the ~150 mV onset shift observed between the 5s deposition and continuous 10s deposition. We hypothesize that the pinched-off junction formed after the initial 5s second deposition was retained because the SiO_2 layer formed during activation prevents the contact area from expanding during the subsequent deposition. Preservation of the pinched-off contacts made the device nearly as efficient after the additional 5s deposition, despite having larger island sizes.

Following the second 5s deposition and additional activation, another 50s deposition was performed on the photoanode for a total of deposition time of 60s. The photocurrent onset potential remains near that of the 5s deposition. The photoanode on which the deposition of nickel was performed sequentially, with activation between depositions, performed significantly better than the photoanode on which a continuous 60s deposition was performed, despite the fact that a similar amount of nickel was deposited on both electrodes. This comparison demonstrates that the pinch-off effect is the primary factor controlling photoanode efficiency, not the coverage of nickel on the surface. It shows photoanodes need not be limited by the often observed tradeoff between stability and efficiency, as pinched-off contacts may be protected, without destroying their rectifying properties.

a)

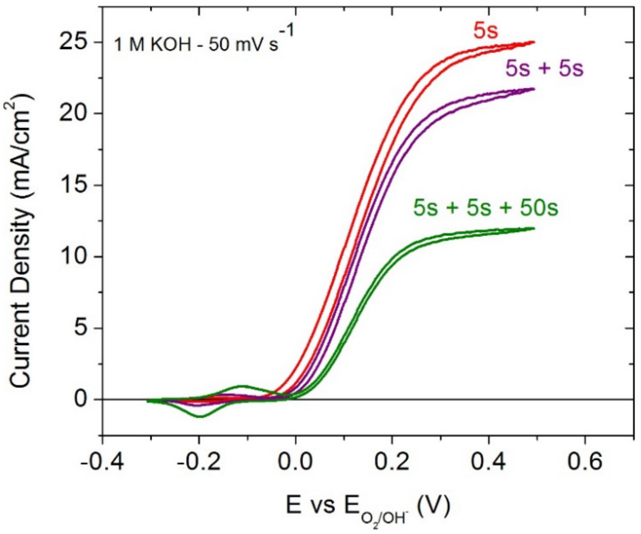
1 M KOH - 50 mV s^{-1}
5s
5s + 5s
5s + 5s + 50s
Current Density (mA/cm^2)
E vs E_{O_2/OH^-} (V)
25
20
15
10
5
0
-0.4
-0.2
0.0
0.2
0.4
0.6

b)

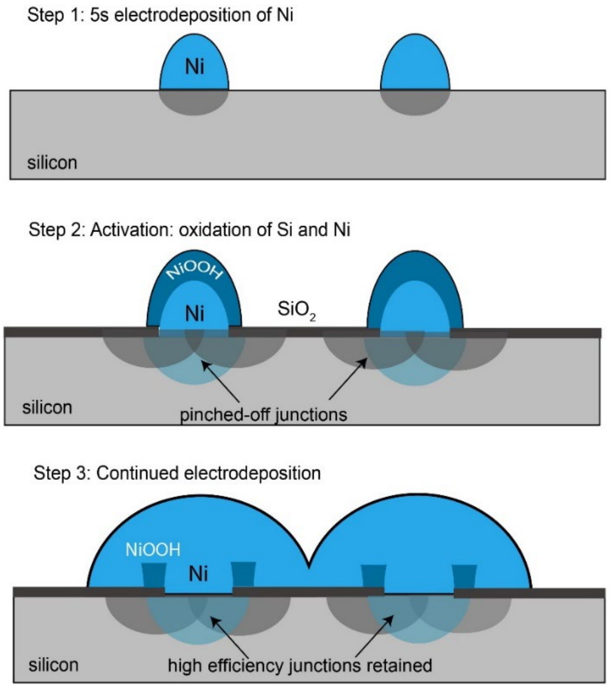
Step 1: 5s electrodeposition of Ni
Ni
silicon
Step 2: Activation: oxidation of Si and Ni
NiOOH
Ni
SiO$_2$
silicon
pinched-off junctions
Step 3: Continued electrodeposition
NiOOH
Ni
silicon
high efficiency junctions retained

c)

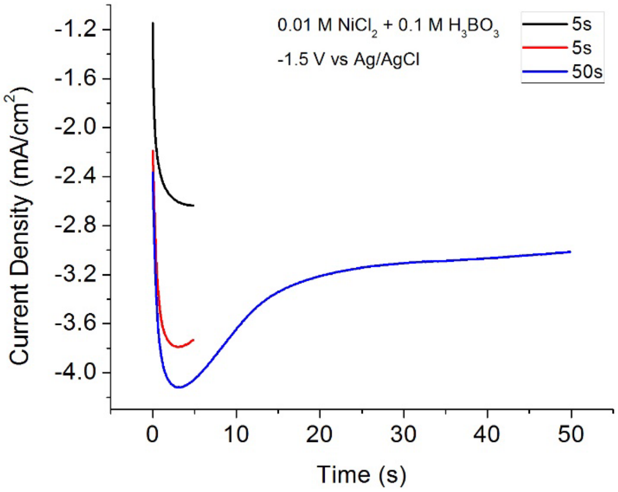

Figure 9. Sequential deposition experiment. a) CVs showing the photocurrent response of the activated photoanode after a 5s nickel deposition + activation, after an addition 5s nickel deposition + activation, and after an additional 50s deposition + activation. Note that after an additional 55s of nickel deposition the photocurrent onset potential shifts only ~70 mV whereas the light limited current is decreased by more than half. b) The sequential deposition process: 5s nickel deposition forms small nickel islands. Activation forms generates NiOOH and SiO_2. The Si-SiO_2-NiOOH interface is retained during further electrodeposition of nickel. c) Deposition curves for the sequential 5s, 5s and 50s depositions.

To test the stability of photoanodes fabricated using the described method of sequential depositions interspersed with activation, we continuously cycled a sequentially deposited photoanode under illumination in 1 M KOH. While the photoanode was cycled, the photocurrent onset potential gradually improved, resulting from further oxidation of Ni to NiOOH which reduces the silicon-nickel contact area. In addition the CVs exhibited multiple redox peaks, most likely due to the presence of both non-pinched-off and pinched-off junctions on the electrode surface. After 500 cycles, which corresponds to approximately 4.4 hours, the light limited current decreased to 75% of its original value. The decrease in light limited current most likely results from oxidation of the surface to non-light-transmitting SiO_2 and NiOOH. This stability test demonstrates that the sequential deposition method does not create a device with the life span needed for commercial use. That the photoanode still does not exhibit reasonable stability after further protection with nickel protection layer suggests that sufficiently stable devices cannot be fabricated with nickel as the protection layer, because of the permeability of nickels catalytically active oxidized form. The amount of nickel that would be needed to completely protect the surface would prevent a significant portion of incident light from hitting the semiconductor surface.

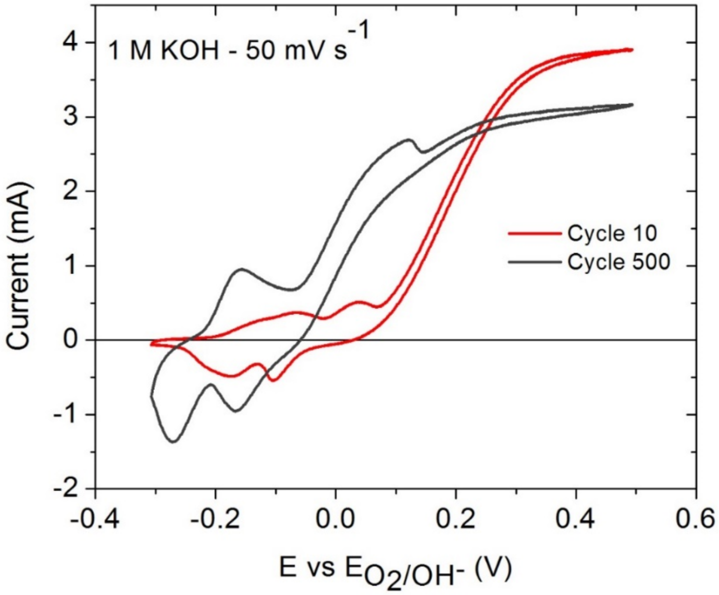

Figure 10. Sequentially deposited electrode stability test. Photocurrent response of the sequentially deposited electrode (5s + 5s + 50s) after 10 and 500 post deposition activation cycles (continuous cycling for over four hours).

Conclusion

Designing a photoanode that can efficiently harness solar energy to drive the oxygen evolution reaction is a major challenge that requires a fundamental understanding of semiconductor-catalyst-solution interfaces. An important area in need of understanding is how the geometry of these interfaces impacts device efficiency. This work shows that the pinch off effect (the enhancement of low barrier height regions by surrounding high barrier height regions) powerfully influences the efficiency of water splitting photoanodes. In addition, we found that photoanodes on which pinched off contacts are initially formed can be coated with additional protection layers, retaining highly efficient contacts while increasing durability. However, devices that rely on a redox active solution-permeable catalyst like nickel show little promise for long-term stability.

The pinch off effect can be used as a guiding principle to design new devices. A possible strategy is to use two materials for the protection layer—one that is protective and another that is catalytically active. A high work function metal could be used to form stable, rectifying contacts on the semiconductor and a catalytically active metal like nickel could be deposited on top of these contacts. Another strategy is to surround nanocontacts with a high work function metal oxide. The electrodeposition method described in this work as well as nanolithography methods provide powerful techniques for fabricating these nanocontacts. Currently, photo water splitting is a technology in the early stages of development. However, with our improved understanding of how charge transfers across interfaces, we can design the top notch devices of the future.

Bibliography

1) Hydrogen Production: Natural Gas Reforming. *Department of Energy*. Available at: https://www.energy.gov/eere/fuelcells/hydrogen-production-natural-gas-reforming. (Accessed: 13th June 2018)

2) Jesper Jacobsson, T., Fjällström F, V., Edoff, M. & Edvinsson, T. Sustainable solar hydrogen production: from photoelectrochemical cells to PV-electrolyzers and back again. (2014). doi:10.1039/c4ee00754a

3) Sze, S. M. & Lee, M.-K. *Semiconductor devices: physics and technology*. (Wiley, 2012).

4) .Fujishima, A, Honda, K Electrochemical Photolysis of Water at a Semiconductor Electrode. *Nature* 238, 37–38 (1972).

5) Kenney, M. J. *et al.* High-performance silicon photoanodes passivated with ultrathin nickel films for water oxidation. *Science* 342, 836–40 (2013).

6) Tan, M. X. *et al. Principles and Applications of Semiconductor Photoelectrochemistry*.

7) Sun, K. *et al.* Stable solar-driven oxidation of water by semiconducting photoanodes protected by transparent catalytic nickel oxide films. *Proceedings of the National Academy of Sciences* 201423034 (2015).

8) Tung, R. T. Electron transport at metal-semiconductor interfaces: General theory. PHYSICAL REVIEW B 45

9) Rossi, Robert C., and Nathan S. Lewis. "Investigation of the size-scaling behavior of spatially nonuniform barrier height contacts to semiconductor surfaces using ordered nanometer-scale nickel arrays on silicon electrodes." *The Journal of Physical Chemistry B*105.49 (2001): 12303-12318.

10) Hill, J. C., Landers, A. T. & Switzer, J. A. An electrodeposited inhomogeneous metal–insulator–semiconductor junction for efficient photoelectrochemical water oxidation. *Nature Materials* 14, 1150–1155 (2015).

11) Laskowski, F. A. L., Nellist, M. R., Venkatkarthick, R. & Boettcher, S. W. Junction behavior of n-Si photoanodes protected by thin Ni elucidated from dual working electrode photoelectrochemistry. *Energy & Environmental Science* 10, 570–579 (2017).

12) Bard, A. J. & Faulkner, L. R. *Electrochemical methods*. (J. Wiley, 1986).

13) Giessibl, F. J. Advances in atomic force microscopy. Rev. Mod. Phys.75,949–983 (2003).

14) Oh, K. *et al.* Elucidating the performance and unexpected stability of partially coated water-splitting silicon photoanodes. *Energy & Environmental Science* 11, 2590–2599 (2018).

15) Yan, Shicheng, et al. "Ni@ Ni (OH) 2 Core-Shell Particles Partially Covering Silicon Photoanode for Enhanced Efficiency and Stability of Photoelectrochemical Water Oxidation." ChemSusChem(2017).

16) Laskowski et al. Nanoscale semiconductor/catalyst interfaces in photoelectrochemistry